Applied Radiation and Isotopes 234 (2026) 112648

Contents lists available at ScienceDirect

Applied Radiation and Isotopes

journal homepage: www.elsevier.com/locate/apradiso

Application of the prompt γ-ray spectroscopy in the boron neutron capture therapy of pets

Victoria D. Maltseva [a,*], Timofey A. Bykov [a,b], Yiliia L. Chesnokova [a], Rahaf Deeb [a,b], Marina A. Degtyareva [c], Ekaterina S. Dmitrieva [c], Anna I. Kasatova [a,b], Dmitrii A. Kasatov [a,b], Iuliia Taskaeva [a,b,d], Sergey A. Uspenskii [e], Sergey Yu. Taskaev [a,b,**]

[a] Budker Institute of Nuclear Physics, Novosibirsk, Russia
[b] Novosibirsk State University, Novosibirsk, Russia
[c] Veterinary Clinic "Doctor Vet", Novosibirsk, Russia
[d] Research Institute of Clinical and Experimental Lymphology, Novosibirsk, Russia
[e] Enikolopov Institute of Synthetic Polymeric Materials, Moscow, Russia

ARTICLE INFO

Keywords:
Boron neutron capture therapy
Prompt γ-ray spectroscopy
Dosimetry
Accelerator-based neutron source
Veterinary oncology

ABSTRACT

Boron Neutron Capture Therapy (BNCT) consists of the selective accumulation of boron-10 in tumor cells and targeted neutron irradiation. A critical challenge for clinical implementation is the accurate real-time measurement of the absorbed boron dose. This study presents the first application of prompt γ-ray spectroscopy to evaluate boron uptake and clearance dynamics during BNCT in a cohort of ten pets with spontaneous tumors. The research was conducted at an accelerator-based neutron source using a high-purity germanium γ-spectrometer, shielded and positioned to detect 478 keV photons emitted during the boron neutron capture reaction. The method successfully allowed for the direct, non-invasive monitoring of boron concentration within the irradiation volume. Results demonstrated significant inter-subject variability, with the intensity of capture reactions differing by a factor of 10 and boron clearance times varying by a factor of 6 among the animals. Crucially, the study established that the measured intensity of boron neutron capture events did not correlate with either tumor volume or boron concentration in the blood. Furthermore, boron clearance from tumors (3–17 h) was notably slower than that from blood (1–3 h). These findings indicate that relying solely on blood analysis for treatment planning is insufficient. Consequently, the integration of prompt γ-ray spectroscopy is strongly recommended for clinical BNCT to ensure precise dosimetry, optimize treatment duration, and improve outcome assessment.

1. Introduction

Boron Neutron Capture Therapy (BNCT) is considered a promising method for treating oncological diseases (Sauerwein et al., 2025; Advances in Boron Neutron Capture Therapy, 2023). It utilizes the uniquely high ability of the non-radioactive boron-10 nucleus to absorb a thermal neutron and the unique property of the nuclear reaction products to deposit almost all of the reaction energy within a small volume – the size of a single cell. The cross-section of the neutron capture reaction by boron $^{10}B(n,\alpha)^{7}Li$ is 3835 b, for a thermal neutron, which is thousands to tens of thousands of times greater than the neutron capture cross-sections of hydrogen, carbon, nitrogen, and oxygen – the atomic nuclei that constitute the human body. The absorption of a neutron by a ^{10}B nucleus leads to an instantaneous nuclear reaction $^{10}B(n,\alpha)^{7}Li$ with the release of 2.79 MeV of energy. In 6.1% of cases, the energy is distributed only between the lithium nucleus and the α-particle; in 93.9% of cases, the lithium nucleus is emitted in an excited state and emits a γ-quantum with an energy of 0.478 MeV. The products of the nuclear reaction – the lithium nucleus and the α-particle are characterized by a short range of these particles in water or body tissue: 5.2 μm and 7.5 μm, respectively. The stopping power for γ-quanta is significantly lower, and its mean free path in water is about 10 cm. Consequently, the deposition of the main part (84%) of the energy from the $^{10}B(n,\alpha)^{7}Li$ nuclear reaction is limited to the size of a single cell.

* Corresponding author.
** Corresponding author. Budker Institute of Nuclear Physics, Novosibirsk, Russia.
E-mail addresses: v.konovalova1@g.nsu.ru (V.D. Maltseva), taskaev@inp.nsk.su (S.Yu. Taskaev).

https://doi.org/10.1016/j.apradiso.2026.112648
Received 24 January 2026; Received in revised form 31 March 2026; Accepted 15 April 2026
Available online 23 April 2026

Thus, the selective accumulation of boron-10 inside tumor cells followed by neutron irradiation should lead to the destruction of tumor cells with relatively minor damage to surrounding healthy cells.

For successful BNCT treatment, it is necessary to: i) deliver boron to tumor cells in a concentration of at least 20 ppm and with a contrast ratio to healthy organ cells of at least 3:1, and ii) irradiate with a flux of epithermal neutrons with an intensity of at least 5×10^8 neutrons/cm^2·s for a period of about 1 h. Currently, the first goal is achieved by using borophenylalanine ((L)-4-dihydroxyborylphenylalanine, BPA), and the second by using a number of accelerator-based neutron sources (Advances in Boron Neutron Capture Therapy, 2023).

One of the main problems requiring solution for the clinical implementation of BNCT is the measurement of absorbed dose, which consists of contributions from the boron dose, the thermal neutron dose, the fast neutron dose, and the γ-ray dose (Sauerwein et al., 2012). The boron dose is due to α-particles and lithium atomic nuclei (products of the ^{10}B(n,α)^{7}Li reaction) – it should be maximized in tumor cells. The thermal neutron dose is due to recoil nuclei from the nuclear reaction of neutron capture by the nitrogen nucleus ^{14}N(n,p)^{14}C. The fast neutron dose is due to recoil nuclei from elastic scattering of neutrons, predominantly fast neutrons, on atomic nuclei, predominantly hydrogen. The γ-ray dose is due to ionization of atoms by γ-rays, whose sources include the charged particle accelerator, the neutron-generating target, the neutron beam shaping assembly, and the irradiated object (patient); these three dose components should be minimized.

The boron dose can be measured directly via the boron neutron capture reaction itself, since in 93.9% of cases one of the reaction products is the emission of a γ-quantum with an energy of 0.478 MeV. By measuring the intensity of 478 keV photon emission, one can determine the number of nuclear reactions that occurred in the observed volume. This method is called the prompt γ-ray spectroscopy and is well-known; its application to BNCT was proposed and described in (Kobayashi and Kanda, 1983). Although this spectroscopy method is well-known, it is practically not implemented. The difficulty lies in the fact that the γ-ray spectrometer must be placed in the neutron flux, have good energy resolution, while photons of the same energy are emitted from the lithium target due to inelastic scattering of protons on lithium nuclei. If a γ-spectrometer relatively resistant to neutron flux is used, its energy resolution will not allow separation of the 478 keV line from the more intense 511 keV line. An HPGe γ-spectrometer separates these lines but is not resistant to neutrons. In other words, attempts to implement this method have been made but have not been successful. Precisely for this reason, significant efforts are directed towards measuring boron concentration (8 methods are described in detail in the book on neutron capture therapy (Sauerwein et al., 2012) in order to reconstruct the boron dose value through numerical modeling of neutron transport.

The aim of this work is to implement technical solutions enabling the practical use of the prompt γ-ray spectroscopy method, to apply this method for measuring boron dose during therapy of large pets with spontaneous tumors, and to develop recommendations for using prompt γ-ray spectroscopy in oncology clinics during BNCT treatment of patients.

2. Experimental facility and measurement methods

Research was conducted at the accelerator-based neutron source at the Budker Institute of Nuclear Physics (Taskaev, 2024). The facility consists of an originally designed tandem electrostatic charged particle accelerator, called a vacuum-insulated tandem accelerator VITA, to obtain a stationary monoenergetic beam of protons or deuterons with energy up to 2.25 MeV, current up to 10 mA; a lithium target for neutron generation; and beam shaping assemblies for forming a neutron beam of the required energy range.

For this study, a proton beam with an energy of 2.05 or 2.1 MeV and a current from 2 to 3 mA was used. The proton beam energy is measured by a resistive voltage divider connected to the high-voltage power supply and calibrated against the threshold reactions ^{7}Li(p,n)^{7}Be and ^{9}Be(p,n)^{9}B. The ion beam current is measured using a target assembly, electrically isolated from the setup, as a deep Faraday cup. A schematic of the experimental facility and equipment used is shown in Fig. 1.

The research aim was to treat pets (cats or dogs) with a spontaneous tumors using BNCT and to apply the prompt γ-ray spectroscopy method for direct detection of photons accompanying the neutron capture reaction by boron, to obtain data on boron accumulation dynamics and boron dose. A total of ten pets participated in the study. Information about the animals and irradiation parameters is presented in Table 1.

An hour prior to irradiation, an intravenous infusion of boron-10 enriched boron-phenylalanine solution (Neuboron Bio-SciTech Co., Ltd., China) with fructose in deionized water was started. The dosage of boron-phenylalanine was 700 mg per kilogram of animal weight, the solution volume was 20 ml per kilogram of animal weight (Sauerwein et al., 2025). In one case (animal No. 5) infusion of the drug was continued during irradiation.

For irradiation, animals were placed directly under the lithium target with the moderator. Initially, a plexiglass disc with a diameter of 200 mm and height of 72 mm was used as the moderator; then, starting from animal No. 9, a polyethylene disc with bulk bismuth inclusions, diameter 155 mm, height 72 mm, was used. This change improved the quality of the neutron beam: the unwanted γ-ray dose rate was reduced by a factor of 2 while maintaining the boron dose rate (Sycheva et al., 2023).

Initially, animals were placed on a raised metal table; starting from animal No. 7, they were placed on a plywood sheet table attached to a controlled robotic arm. Fig. 2 shows a photograph of an animal placed for irradiation on a plywood sheet table held by a robotic arm, under the lithium target with a polyethylene moderator containing bulk bismuth inclusions.

The key solution enabling the implementation of the prompt γ-ray spectroscopy method was to place the γ-spectrometer as far as possible from the irradiation zone and protect it from neutrons as much as possible. To achieve this, the γ-spectrometer was placed in an adjacent radiation-shielded room (bunker 2) behind a 1.5 m thick concrete wall.

A 100 mm diameter hole was drilled in the wall to register radiation from the irradiation object. A collimator made of 50 mm thick lead bricks with a dovetail profile was placed in front of the animal – first movable (Fig. 3a), then, starting from the 7th animal, fixed (Fig. 3b). The collimation aperture size for animals No. 1 and 6-10 was 25 mm wide by 50 mm high; for animals No. 2-4 it was 12 mm wide by 50 mm high; for animal No. 5, no collimator was used. The height of the collimator was set to the size of a brick, the width – the purpose of the study. A narrow collimator (12 mm) was used to study the spatial distribution of boron, a wider one (25 mm) – the temporal one.

To suppress neutron penetration into bunker 2, a 12 mm thick plexiglass plate, providing neutron scattering, was installed in front of the wall hole in bunker 1. A similar plexiglass plate was installed in bunker 2 in front of the spectrometer. The spectrometer detector was wrapped in 0.1 mm cadmium foil to absorb thermal neutrons to ensure better safety of the spectrometer. The spectrometer detector was placed inside a lead collimator to reduce background signal and detector load.

Measurements were performed using the SEG-1KP HPGe γ-spectrometer (Institute of Physics and Technology, Dubna) based on a semiconductor detector made of high-purity germanium (HPGe γ-spectrometer) (SEG-1KP). A crystal of high-purity germanium has the shape of a cylinder with a diameter of 90 mm and height of 85 mm. Initially, a spectrometer with a measurement range up to 2 MeV was used; then, starting from animal No. 9, a spectrometer with a range up to 10 MeV was used. The use of a spectrometer with a wide range of measured energies made it possible to measure the intensity of the 2.223 MeV line caused by the capture of a neutron by hydrogen in the ^{1}H(n,γ)^{2}H reaction; the intensity of this line is proportional to the volume of tissue in the detection area.

According to specifications, the energy resolution of the HPGe

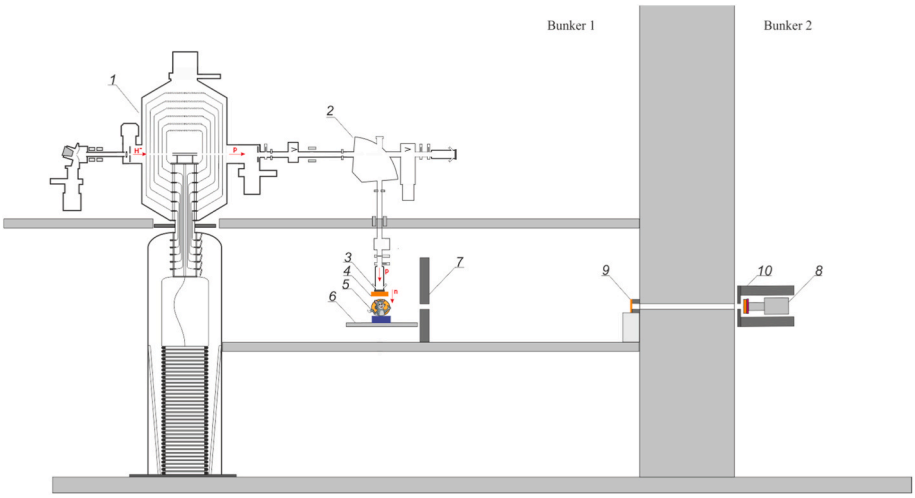

Fig. 1. Schematic of the experimental facility: *1* – vacuum-insulated tandem accelerator, *2* – bending magnet, *3* – lithium neutron-generating target, *4* – moderator, *5* – irradiation object, *6* – table for placing the irradiation object, *7* – lead collimator, *8* – γ-spectrometer, *9* – neutron scatterer, *10* – spectrometer lead collimator.

Table 1
Animal information and irradiation parameters (*V* – tumor volume, Φ – proton fluence, *E* – proton energy).

№	Date of treatment	Gender	Species	Breed	Age (years)	Weight, kg	Type of tumor	*V*, g	Φ, mA·h	*E*, MeV
1	27.06.23	F	cat	half-breed	9	4	adenocarcinoma in the nasal cavity	8	4.4	2.05
2	05.10.23	M	cat	half-breed	6	4,3	adenocarcinoma in the nasal cavity	6	4.4	2.05
3	05.10.23	F	cat	half-breed	18	2,9	mandibular cancer, left side	7	4.4	2.05
4	05.10.23	F	cat	half-breed	14	3,3	poorly differentiated carcinoma of the nasal cavity	8	4.4	2.05
5	20.10.23	F	dog	yorkshire terrier	8	4,2	lung cancer with metastases		4.4	2.05
6	01.03.24 09.04.24	M	cat	maine coon	14	8	soft tissue sarcoma of the right cheek	16	0.85 2.25	2.05 2.05
7	26.09.24	M	dog	tibetan spaniel	13	8	adenocarcinoma in the nasal cavity	5	4.4	2.05
8	05.12.24	F	cat	half-breed	10	4,8	soft tissue sarcoma of the right cheek	8	4.4	2.05
9	22.09.25	F	cat	bengal cat	8	4	fibrosarcoma of the maxilla	8.9	3.7	2.1
10	22.09.25	M	cat	half-breed	13	4,6	osteosarcoma of the mandible	12.7	3.7	2.1

Fig. 2. Photograph of an animal positioned for irradiation.

γ-spectrometer detector is 1.4 keV for the ^{57}Co emission line at 122 keV and 3.5 keV for the ^{60}Co emission line at 1332 keV. Calibration of the HPGe γ-spectrometer detector for energy and detection efficiency was performed using 12 radiation sources (two powerful, seven from the OSGI RT set, and three self-made) and was described in detail in (Bikchurina et al., 2021). The detection efficiency for the 478 keV line is given by $\varepsilon = 55.5/x^2$, where x is the distance from the radiation source to the detector; in this case $x = 6471$ mm for the spectrometer with range up to 2 MeV and $x = 7143$ mm for the spectrometer with range up to 10 MeV.

Before the study involving pets, the created spectrometric complex was tested with a cesium-137 γ-ray source type IGI Ts 3 1 (Mayak, Ozyorsk, Chelyabinsk region) and with boric acid solutions with boron-10 concentrations from 10 μg/ml to 200 μg/ml (Bikchurina et al., 2023).

3. Results

3.1. Case No. 1

The prompt γ-ray spectroscopy method was first applied during the treatment of the cat on June 27, 2023. Fig. 4 shows a characteristic spectrum of the detected radiation. The 478 keV photon line is broadened and reliably measurable. Such good registration of photons from the ^{10}B(n,α)^{7}Li reaction is ensured by almost complete suppression of monochromatic 478 keV photons from the lithium target in the ^{7}Li(p, p'γ)^{7}Li reaction due to shielding of the lithium target with lead bricks and significant suppression of the neutron flux by placing plexiglass scatterers and cadmium foil.

Note other lines in the measured spectrum. The 511 keV line is due to annihilation processes; the 517 keV line is due to neutron capture by chlorine ^{35}Cl(n,γ)^{36}Cl, and its intensity is proportional to the volume of tissue in the detection region; the 558 keV line is due to neutron capture

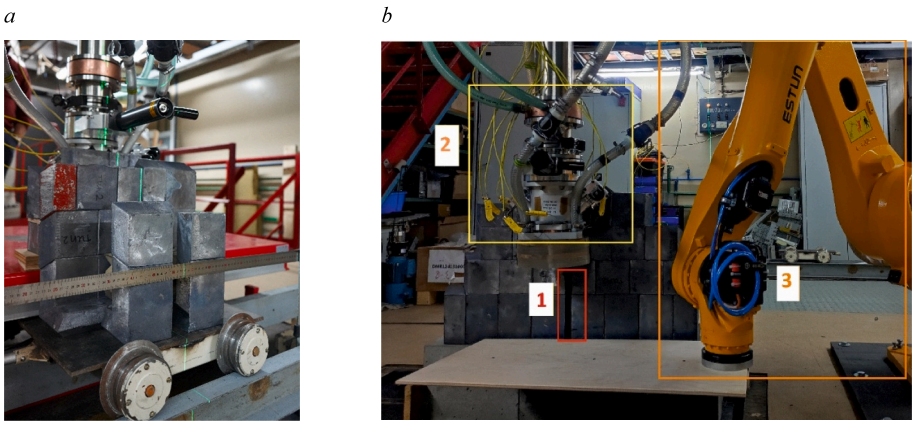

Fig. 3. Collimator: *a*) movable, *b*) stationary: *1* – collimation aperture, *2* – lithium target, *3* – robotic arm holding the table.

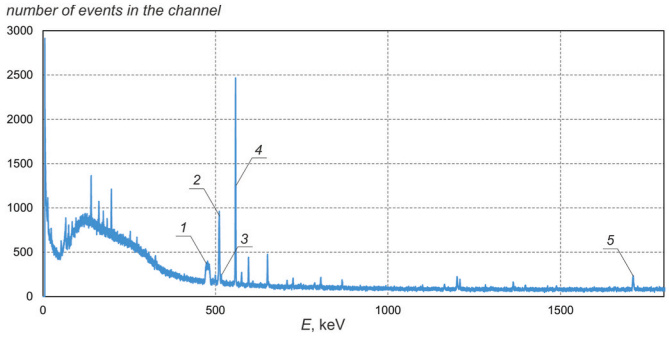

Fig. 4. Characteristic energy spectrum measured by the γ-spectrometer: *1* – 478 keV, *2* – 511 keV, *3*– 517 keV, *4* – 558 keV, *5* – 1712 keV.

by cadmium $^{113}Cd(n,\gamma)^{114}Cd$, which wraps the spectrometer detector, its intensity is proportional to the number of neutrons scattered from the detection region; the 1712 keV line is the single-escape peak for the 2.223 MeV line emitted during neutron capture by hydrogen $^{1}H(n,\gamma)^{2}H$, and its intensity is also proportional to the volume of tissue in the detection region. It should be noted that the measurement error for the number of counts in a line depends on many factors (detector sensitivity, detector load, count rate, background signal, etc.) and is estimated at 10%.

Irradiation was conducted for 2 h with two interruptions. The first interruption of 4 min was needed to restart the turbomolecular pump, the second of 22 min to reposition the animal. Eleven measurements were taken during irradiation; main parameters are in Table 2.

Table 2
Gamma-spectrometer measurement parameters.

Measurement start time	Measurement end time	Total time, ms	Live time, ms	Proton fluence, mA·h	The number of events in the 478 keV line
13:23:16	13:37:32	853172	744888	0.4358	20480
13:37:39	13:49:44	722972	617071	0.4358	19042
13:49:49	13:55:20	328798	282182	0.1943	8056
13:59:26	14:06:06	397291	339434	0.2393	9854
14:06:13	14:19:22	786516	670431	0.4688	18933
14:19:30	14:29:53	620492	526008	0.3867	15323
14:51:31	15:04:32	778765	687242	0.4346	11887
15:04:38	15:17:03	743329	651004	0.4481	12238
15:17:12	15:29:02	708684	622024	0.4234	10876
15:29:09	15:41:20	729001	624069	0.4343	10926
15:41:27	15:53:34	724477	601199	0.4358	9719

The measurement results allow reconstruction of the temporal dynamics of the boron dose rate, which is proportional to the amount of boron in the detection region; it is shown in Fig. 5. Initially, the animal's head was positioned so that the tumor in the nasal cavity was in direct line of sight of the γ-spectrometer; after repositioning, the tumor was obscured by the head. Photon attenuation in the animal's head resulted in a 1.4-fold decrease in the recorded signal. Applying this correction yields a graph of smooth decrease in dose rate with a characteristic time of 6.6 h (time for the signal to decrease by a factor of *e*).

Let's estimate the absorbed dose from the $^{10}B(n,\alpha)^{7}Li$ reaction. A total of 147 000 counts were registered in the 478 keV photon line, as follows from Table 2. Considering the correction and taking into account that the spectrometer registered 86% of the irradiation time (live time to total time ratio; see Table 2), we find that during irradiation 197 000 photons should have reached the γ-spectrometer detector from the tumor. Under the assumption of isotropic photon emission and an absolute detection efficiency of $1.31{\cdot}10^{-6}$ for the detector placed at a distance of 6471 mm from the irradiation region, we find that during irradiation $1.5{\cdot}10^{11}$ photons were emitted from the tumor as products of the $^{10}B(n,\alpha)^{7}Li$ reaction. Since the $^{10}B(n,\alpha)^{7}Li$ reaction proceeds with photon emission in 93.9% of cases and without emission in 6.1%, the total number of $^{10}B(n,\alpha)^{7}Li$ reactions is $1.6{\cdot}10^{11}$. As 2.34 MeV is released in the tumor cell as a result of the nuclear reaction, such a number of reactions leads to the release of energy equal to 60 mJ. Based on computed tomography data, the tumor volume of the animal is estimated at 8 cm^3. Under the assumption of tumor-specific boron uptake we obtain an absorbed boron dose value of 7.5 Gy or 28.5 Gy equivalent, assuming a compound biological effectiveness factor of 3.8.

Of course, boron accumulates not only in tumor cells but also in healthy cells at a 3-4 times lower concentration. Precise measurement of accumulation selectivity is a complex task. Repositioning the animal during its therapy led to a definitive result, confirming tumor-selective boron accumulation.

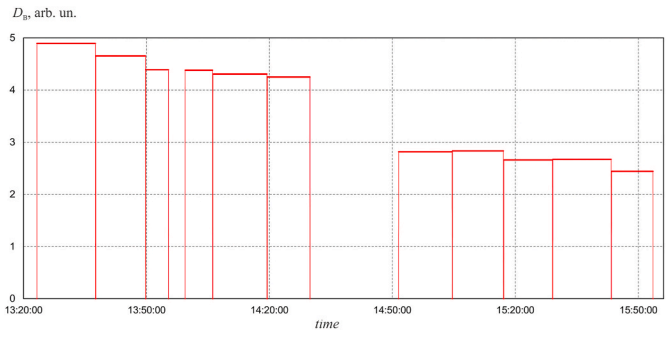

Fig. 5. Time dynamics of the measured boron dose rate, D_B.

3.2. Cases No. 2-4

The next irradiation of three animals was performed on the same day. The research aim was to test the possibility of measuring the spatial distribution of boron accumulation by shifting the collimator horizontally. The collimator with a 12 mm wide aperture was first placed in the center, then shifted left, then returned to center and shifted right.

The data in Fig. 6, obtained from a collimator position scan, show the intensity of the 478 keV emission line (correlated with boron uptake) and the 558 keV cadmium line (whose signal is proportional to scattered neutrons and provides a measure of tissue volume, as detailed later). In all cases, the proton fluence was 0.435 mA h. The graphs also show the ratio of these signals, which is proportional to boron concentration in the tissue.

The effect of selective boron accumulation in tumor cells was most pronounced during therapy of animal No. 2 (Fig. 6a and b). It is seen that the highest signal in the 478 keV line was registered at collimator position +12 mm. When the collimator is moved to the left, the signal in the 478 keV line decreases, while the signal in the 558 keV line remains approximately constant. At the same time, when the collimator is shifted to the right, the signal in the 478 keV line decreases, while the 558 keV signal exhibits an approximate two-fold increase as the sampled tissue volume increases. Looking at the ratio of these signals (ratio of the 478 keV signal to the 558 keV signal divided by 6), selective boron accumulation in the tumor is clearly seen for animal No. 2 (Fig. 6b), less pronounced for animal No. 3 (Fig. 6d), and intermediate for animal No. 4 (Fig. 6f).

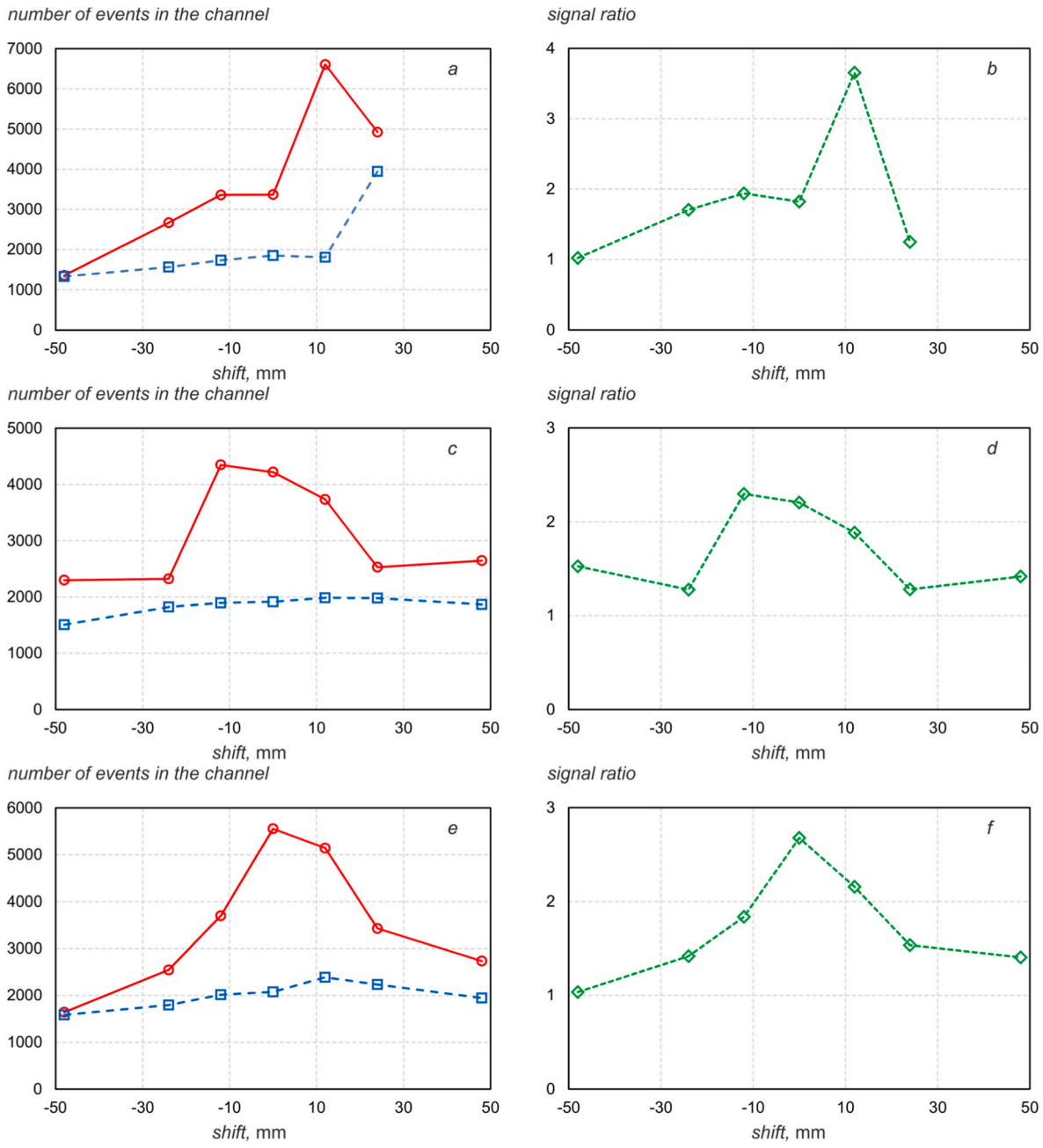

Fig. 6. Integrated counts under the 478 keV line (◯), the 558 keV line divided by 6 (□), and their ratio (⋄) as a function of collimator offset at a proton fluence of 0.435 mA h. Panels: *a*, *b*) animal № 2; *c*, *d*) animal №3; *e*, *f*) animal №4.

3.3. Case No. 5

During the treatment of animal No. 5 with a lung tumor and metastases, the collimator was not used, and the infusion of the boronophenylalanine (BPA) drug was continued during irradiation. Fig. 7 shows the time dependence of the event count in the 478 keV line, normalized to a proton fluence of 1 mA h. It can be seen that continuing the BPA infusion leads to boron accumulation. Approximately in the middle of the irradiation, the solution was exhausted, and the boron content began to decrease. Considering the signal drop rate based on the last five measurement points, the signal reduction time by a factor of *e* is 9 h.

Note that in this plot and in the plots presented below, the signal is zero for several time intervals. A period of 5-10 s was required for data saving after stopping a measurement and launching the program for a new measurement. Longer intervals with a zero signal are associated either with a temporary pause in irradiation or with a delay in launching the measurement program.

3.4. Case No. 6

Animal No. 6 was irradiated twice with boronophenylalanine (BPA) infusion due to a malfunction of the accelerator's injector. During the first irradiation, the animal received approximately 20% of the planned dose; during the second irradiation, an additional 50%, totaling 70%. It was not possible to achieve the planned dose due to the low ion current provided by the injector and, consequently, the prolonged irradiation time, as well as due to the rapid boron elimination.

Fig. 8 presents the time dependence of the 478 keV line event count (normalized to a proton fluence of 1 mA h) during the second irradiation. Among all irradiated animals, in case of this animal, characterized by rapid tumor growth, the highest photon yield was recorded, indicating the greatest boron accumulation in the tumor. The graph also shows a rapid decline in boron accumulation; the signal reduction time by a factor of *e* is 3 h.

The day before the first irradiation with boronphenylalanine infusion, we performed an additional short irradiation of the animal that had been injected with boron nanoparticles (without BPA). These boron nanoparticles had previously demonstrated good cellular uptake (Uspenskii et al., 2020; Zaboronok et al., 2022), which led to the decision to test them for treatment. These elemental boron nanoparticles with natural isotopic abundance were synthesized via ultrasonic processing of isotopes in an aqueous medium and had a size of 70 ± 10 nm. For infusion, a dispersion of elemental boron nanoparticles in hyaluronic acid was prepared at a concentration of 500 μg/ml. The infusion of the boron nanoparticle solution began 1 h 15 min before irradiation and was stopped prior to irradiation.

The irradiation was carried out at a proton energy of 2.05 MeV for 12 min 38 s, up to a proton fluence of 0.1 mA h. The accumulated integral in the 478 keV line was 2093 events. This line intensity was lower

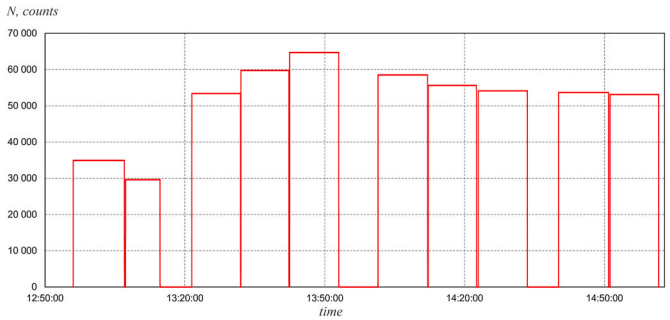

Fig. 7. Dependence of the 478 keV line event count N (normalized to a proton fluence of 1 mA h) on time during the irradiation of animal No. 5.

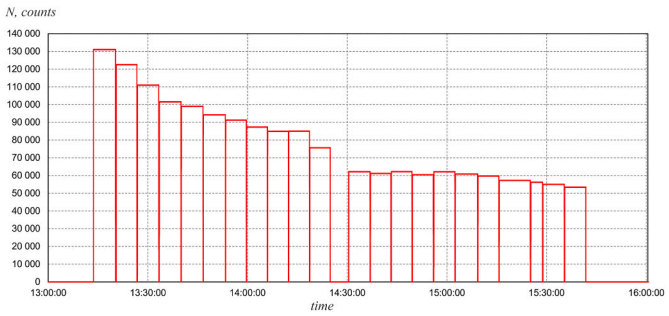

Fig. 8. Dependence of the 478 keV line event count N (normalized to a proton fluence of 1 mA h) on time during the irradiation of animal No. 6.

than the optimal one for treatment, and the irradiation was stopped. Nevertheless, it should be noted that this level of boron accumulation should be considered extremely successful. If the boron nanoparticles had been fabricated using boron enriched with the boron-10 isotope, the signal would have been 5 times greater, amounting to approximately 100 000 events per 1 mA h. This intensity is comparable to the radiation intensity presented in Fig. 8 and greater than the obtained during the treatment of subsequent animals.

Thus, the first application of elemental boron nanoparticles for treatment of animals can be considered quite successful, and studies with elemental boron nanoparticles enriched with the boron-10 isotope should be continued.

3.5. Cases No. 7 and 8

During the irradiation of animals No. 7 and 8, a stationary collimator was used, and at the end of the irradiation, the table with the animal was moved parallel to the collimator.

Fig. 9 presents the time dependence of the 478 keV line event count (normalized to a proton fluence of 1 mA h) during the irradiation of animal No. 7. The last five data points, starting at time 15:13:02, correspond to measurements taken while the table with the animal was being moved parallel to the collimator – first 2.5 and 5 cm to the right, then 2.5, 5, and 7.5 cm to the left.

In this case, healthy organs were the main radiation source, and the signal from them was significantly lower, indicating less boron accumulation in healthy organ cells (the signal in the 558 keV line changed insignificantly, within 5%). Before the animal's repositioning started, the plot indicates a very slow decline in boron concentration, with an estimated e-folding time of 17 h.

Fig. 10 shows the time dependence of the number of events in the 478 keV line, normalized to a proton fluence of 1 mA h, during the irradiation of animal No. 8. The last five data points, starting at time 17:31:32, correspond to measurements taken while the table with the animal was moved parallel to the collimator – first 2.5 cm to the right (towards the animal's head), then 2.5, 5, and 7.5 cm to the left, and

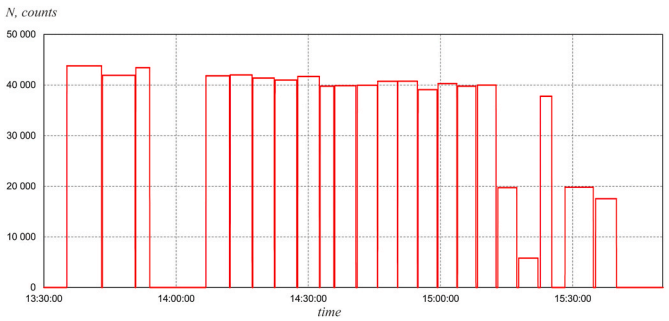

Fig. 9. Dependence of the 478 keV line event count N (normalized to a proton fluence of 1 mA h) on time during the irradiation of animal No. 7.

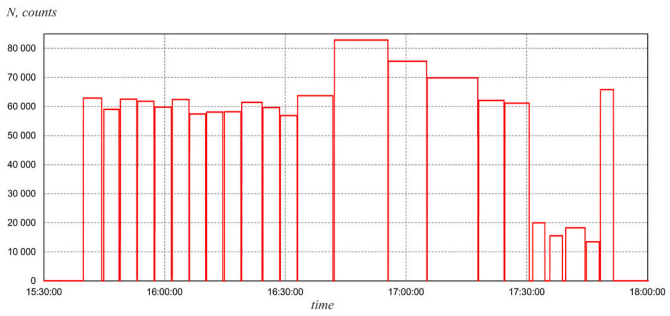

Fig. 10. Dependence of the 478 keV line event count N (normalized to a proton fluence of 1 mA h) on time during the irradiation of animal No. 8.

returned to the initial position.

It can be seen that in the second half of the irradiation time, the signal in the 478 keV line increased. This change is due to the animal moving on its own, causing the spectrometer to observe a different area with a higher boron concentration. With this movement of the animal, the signals in the 558 keV line (cadmium line) and the 1712 keV line (hydrogen line) also increased, indicating that the volume of the animal's mass within the observation area increased. By dividing the radiation intensity in the 478 keV line by the intensity in the cadmium or hydrogen lines, information about the average boron content in the observation area has been obtained. The temporal evolution of the 478 keV/558 keV intensity ratio is presented in Fig. 11. It can be seen that the boron content decreases over time, and the signal reduction time by a factor of *e* can be estimated as 9 h.

During the animal's movement, the spectrometer was focused primarily on healthy organs. As can be seen in Fig. 11, the measured boron concentration decreased by a factor of 2-3, indicating selective boron accumulation in tumor cells.

Starting from animal No. 7, double blood sampling was performed: before the start of irradiation and after its completion for boron concentration analysis. The boron concentration in the blood was determined by inductively coupled plasma atomic emission spectrometry. Sample preparation was carried out using concentrated nitric acid (high-purity grade, 69%) and hydrogen peroxide (37%), heating to 90 °C until dissolution and the formation of a clear solution. Boron concentration was determined using a high-resolution ICPE–9820 spectrometer (Shimadzu, Japan). The measurement results are presented in Table 3.

3.6. Cases No. 9 and 10

In the case of animals 9 and 10, irradiation was performed with a static collimator and without displacement of the animal stage. Also, for the first time, a γ-spectrometer with a measurement range up to 10 MeV was used. As the spectrometer was placed at a longer distance, its sensitivity decreased by a factor of 1.22. Because a polyethylene moderator with a volumetric bismuth inclusion was used, which

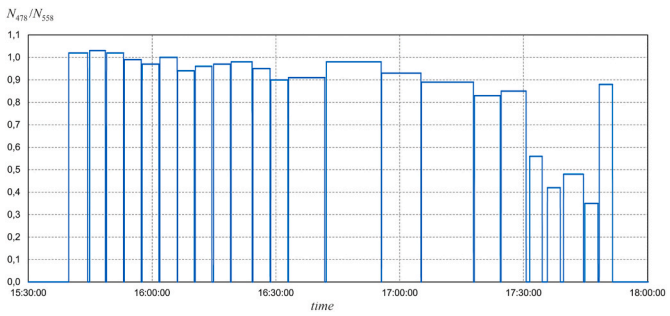

Fig. 11. Time-dependent ratio of the 478 keV (N_{478}) to the 558 keV (N_{558}) line intensities for animal No. 8.

Table 3
Boron-10 concentration in animal blood.

Pets	Concentration of boron in the blood, μg/g	
	before irradiation	after irradiation
№ 7	32.0	14.6
№ 8	59.6	25.0
№ 9	50.8	11.5
№ 10	84.5	28.5

significantly reduces the γ-ray dose while preserving the boron dose, the proton energy was increased from 2.05 MeV to 2.1 MeV. In this case, the fast neutron dose rises a bit more than the therapeutic boron dose, but this is permissible since the undesirable γ-ray dose was reduced. This elevation in proton energy enhances the neutron yield by a factor of 1.335, and at a proton fluence of 3.7 mA h, the boron dose under the same parameters will be 12% greater than that at a proton energy of 2.05 MeV and a fluence of 4.4 mA h.

During the irradiation of animal No. 9, the radiation intensity in the 478 keV line was extremely low. The time dependence of the number of events in the 478 keV line, normalized to a proton fluence of 1 mA h and multiplied by 0.914, is presented in Fig. 12. The coefficient 0.914 was obtained by multiplying by 1.22 to compensate for the decrease in the spectrometer detector's sensitivity due to its relocation to a greater distance and dividing by 1.335 due to the increase in neutron yield when raising the proton energy from 2.05 to 2.1 MeV. This correction allows for a comparison of the measured intensity results for the irradiation of the last two animals with those obtained earlier. The signal reduction time by a factor of *e* is estimated to be 6 h.

Fig. 13 shows the time dependence of the 478 keV line event count, normalized to a proton fluence of 1 mA h and multiplied by 0.914, during the irradiation of animal No. 10. A clear initial increase in the 478 keV signal intensity is observed (a similar trend was noted for animal No. 9) and then decreases, the signal *e*-folding time is estimated at 6 h.

Analysis of a post-treatment X-ray (Fig. 14), obtained one month later, demonstrated that the tumor volume decreased 26-fold, declining from 12.7 g to 0.48 g.

Previously, we assumed that the intensity of the cadmium line (558 keV) is proportional to the volume of the animal's body within the field of detector's view. This assumption was supported by comparing it with the intensity of the 1712 keV line – the single-escape peak of the 2.223 MeV line emitted in the neutron capture reaction $^{1}H(n,\gamma)^{2}H$. In this case, using a spectrometer with a measurement range up to 10 MeV opened up the possibility to directly compare the intensity of the 558 keV line with that of the 2.223 MeV line; their ratio is 0.445 ± 0.14. Therefore, the cadmium line intensity can be considered proportional to the hydrogen line intensity and can be used for the assessment of boron concentration.

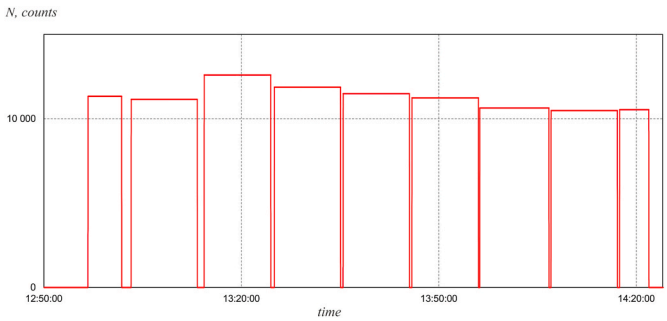

Fig. 12. Dependence of the 478 keV line event count N (normalized to a proton fluence of 1 mA h and multiplied by 0.914) on time during the irradiation of animal No. 9.

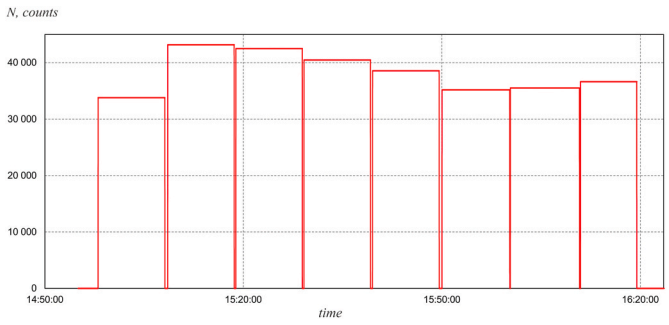

Fig. 13. Dependence of the 478 keV line event count N (normalized to a proton fluence of 1 mA h and multiplied by 1.22) on time during the irradiation of animal No. 10.

4. Discussion

In this work, we refrain from providing a clinical assessment of the treatment outcomes. However, we can note that BNCT invariably led to tumor reduction and consistently resulted in an improvement in the animal's condition. Nevertheless, owners were often compelled to euthanize their pets, mainly due to the fact that because the animals arrived at our laboratory in severe or critical condition and at an advanced age.

We also refrain from a quantitative dose evaluation in this study, as we consider this task exceedingly complex, both in terms of measuring the absorbed dose and determining the equivalent (biological) dose.

The study involved ten pets, the majority weighing between 4 and 5 kg (maximum weight 8 kg, minimum 2.9 kg) with spontaneous tumors weighing between 5 and 16 g, predominantly located in the head region.

Key results obtained during the treatment of the animals are collated in Table 4.

A significant inter-animal variation is observed for two key parameters: the 478 keV line intensity (boron neutron capture reaction count), differing by a factor of 10 (from 13 000 to 130 000 counts, on average 50 000 ± 35 000 counts), and its *e*-folding reduction time (the time of boron removal from the tumor), differing by a factor of 6 (from 3 to 17 h, on average 8 ± 4 h).

It should be stated that the measured intensity of boron neutron capture reactions correlates with neither the tumor volume nor the blood boron concentration. This is a somewhat unexpected result, as in human treatment planning, the boron concentration in the tumor is assumed to be proportional to its concentration in blood. In two Japanese clinics treating patients, the tumor boron concentration is estimated to be three times higher than in blood. At a clinic in Xiamen (China), positron emission tomography data are used, and the tumor boron concentration is also estimated to be several times higher than in blood, with the factor varying from patient to patient. Attention should also be drawn to the differing dynamics of boron clearance from the tumor (ranging from 3 to 17 h) and from the blood (ranging from 1 to 3 h).

There are many potential factors that can cause interindividual variability in boron dynamics. To clarify this, we plan to conduct additional studies in 10 pets, limiting the diversity of tumors and restricting the study design. We will try to treat pets with adenocarcinoma and use a mobile collimator to determine the time dynamics of boron accumulation in the tumor, in healthy tissue, and in the kidneys. We will also try to evaluate the therapeutic effect using ongoing assessment of animal condition.

The obtained data indicate that for therapy planning and outcome assessment, the prompt γ-ray spectrometry method is strongly recommended for treating patients with malignant tumors using BNCT.

We recommend using a high-energy-resolution γ-spectrometer, such as an HPGe detector, and placing it outside the irradiation room in an area of low neutron flux. We propose incorporating the following additional features into the treatment planning system (dosimetry planning system): within the field of view, it should calculate the number of neutron capture reactions by boron-10 $^{10}B(n,\alpha\gamma)^{7}Li$, the

Table 4
The primary outcomes of the animal therapy: tumor mass *m* (if known); peak intensity *I* of radiation of the 478 keV line normalized to a proton fluence of 1 mA h, measured with a 2.5 cm × 5 cm collimator (a correction factor of 2.08 is applied for data obtained with a 1.2 cm × 5 cm collimator); The *e*-folding reduction time *T* of the 478 keV emission line intensity; boron concentration *n* in blood before irradiation and The *e*-folding reduction time T_b of the boron concentration in blood (interval between blood samplings equals the irradiation time plus 20 min).

Pet	*m*, g	*I*, counts	*T*, h	*n*, μg/g	T_b, h
1	8	47 000	6.6		
2	6	32 000	-		
3	7	21 000	-		
4	8	27 000	-		
5		-	9		
6	16	131 000	3		
7	5	44 000	17	32.0	3
8	8	83 000	9	59.6	3
9	8.9	13 000	6	50.8	1
10	12.7	47 000	6	84.5	1.5

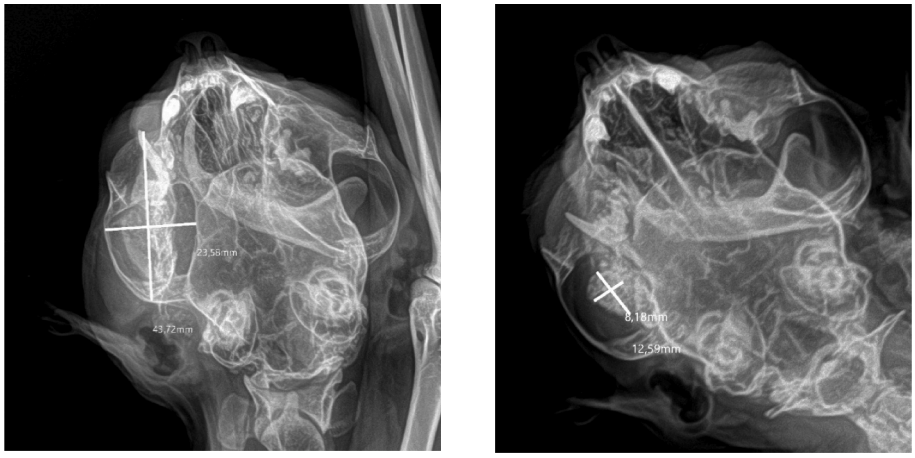

Fig. 14. X-ray images of animal No. 10 before irradiation (*a*) and one month after irradiation (*b*).

number of neutron capture reactions by hydrogen $^{1}H(n,\gamma)^{2}D$, the attenuation coefficient for the 478 keV photon flux in the direction of the γ-spectrometer, and the attenuation coefficient for the 2.223 MeV photon flux in the direction of the γ-spectrometer (Berendeev et al., 2025). Comparison of calculated and measured quantities of nuclear neutron absorption reactions by hydrogen $^{1}H(n,\gamma)^{2}D$, accounting for the attenuation of the 2.223 MeV photon flux in the direction of the γ-spectrometer placement, provides reliable verification of the neutron flux. Similarly, comparison of the calculated and measured numbers of nuclear neutron capture reactions by boron, $^{10}B(n,\alpha\gamma)^{7}Li$, accounting for the attenuation of the 478 keV photon flux in the direction of the γ-spectrometer placement, provides reliable determination of the boron concentration. This is important for treatment planning, determining the treatment duration, and evaluating the outcome.

For the calibration of the γ-spectrometer, we propose using a lithium target as a radionuclide source of 478 keV photons. During patient therapy, the radioactive isotope beryllium-7 is produced in the target upon irradiation with a proton beam via the nuclear reaction $^{7}Li(p,n)^{7}Be$ (Kasatov et al., 2025). The resulting beryllium nuclei decay with a half-life of 53.22 days, emitting a 478 keV photon. The photon energy from this radionuclide source matches the energy of photons detected by the γ-spectrometer for boron dose measurement. Furthermore, the intensity of this photon source is comparable to the intensity of the emission measured by the γ-spectrometer for boron dose measurement.

5. Summary and conclusion

This work presents the results of the first application of prompt γ-ray spectrometry to evaluate boron uptake and clearance during boron neutron capture therapy (BNCT) in a cohort of ten pets. It is demonstrated that the intensity of boron neutron capture nuclear reactions and the boron clearance time differ significantly in different animals: the former by a factor of 10, and the latter by a factor of 6. It has been established that there is no correlation between the measured intensity of boron neutron capture events and either boron concentration in tumor volume or blood. The implementation of prompt γ-ray spectrometry is advised in boron neutron capture therapy (BNCT) for patients with malignant tumors for therapy planning, in determining its duration, and in assessing its outcome. Furthermore, it is recommended to integrate additional functionality into the treatment planning system for calculating in the field of view: the number of $^{10}B(n,\alpha\gamma)^{7}Li$ reactions, the number of $^{1}H(n,\gamma)^{2}H$ reactions, the attenuation coefficient for the 478 keV photon flux towards the γ-spectrometer, and the attenuation coefficient for the 2.223 MeV photon flux towards the γ-spectrometer.

Institutional Review Board Statement: The study was conducted according to the guidelines of the Declaration of Helsinki and approved by the Institutional Review Board of the Center for Genetic Resources of Laboratory Animals, Institute of Cytology and Genetics SB RAS, Novosibirsk, Russian Federation (protocol #91, "Boron neutron capture therapy in domestic cats and dogs", 05.10.2021), and all manipulations were performed while respecting the principles of the humane treatment of animals (European Community Directive 86/609/EEC).

CRediT authorship contribution statement

Victoria D. Maltseva: Data curation, Formal analysis, Investigation, Validation, Writing – original draft. **Timofey A. Bykov:** Investigation, Software, Visualization. **Yiliia L. Chesnokova:** Data curation, Project administration, Visualization. **Rahaf Deeb:** Investigation, Visualization. **Marina A. Degtyareva:** Conceptualization, Resources, Supervision, Writing – review & editing. **Ekaterina S. Dmitrieva:** Formal analysis, Investigation, Resources, Writing – review & editing. **Anna I. Kasatova:** Data curation, Formal analysis, Validation, Writing – original draft. **Dmitrii A. Kasatov:** Conceptualization, Methodology, Validation, Visualization, Writing – review & editing. **Iuliia Taskaeva:** Formal analysis, Supervision, Validation. **Sergey A. Uspenskii:** Methodology, Resources, Validation, Writing – review & editing. **Sergey Yu. Taskaev:** Conceptualization, Funding acquisition, Project administration, Supervision, Writing – review & editing.

Declaration of competing interest

The authors declare that they have no known competing financial interests or personal relationships that could have appeared to influence the work reported in this paper.

Data availability

Data will be made available on request.

References

Advances in Boron Neutron Capture Therapy, 2023. International Atomic Energy Agency, Vienna, Austria, p. 416.

Berendeev, E., Koshechkin, S., Koshkarev, A., Shein, T., Taskaev, S., 2025. The method for planning boron neutron capture therapy and evaluating its outcome. Patent for invention RU 2850118. (Accessed 5 November 2025).

Bikchurina, M., Bykov, T., Ibrahim, I., Kasatova, A., Kasatov, D., Kolesnikov, Ia, Konovalova, V., Kormushakov, T., Koshkarev, A., Kuznetsov, A., Porosev, V., Savinov, S., Shchudlo, I., Singatulina, N., Sokolova, E., Sycheva, T., Taskaeva, I., Verkhovod, G., Taskaev, S., 2023. Dosimetry for boron neutron capture therapy developed and verified at the accelerator based neutron source VITA. Front. Nucl. Eng. 2, 1266562. https://doi.org/10.3389/fnuen.2023.1266562.

Bikchurina, M., Bykov, T., Kasatov, D., Kolesnikov, Ia, Makarov, A., Shchudlo, I., Sokolova, E., Taskaev, S., 2021. The measurement of the neutron yield of the 7Li(p, n)^{7}Be reaction in lithium targets. Biology 10, 824. https://doi.org/10.3390/biology10090824.

Kasatov, D., Konovalova, V., Taskaev, S., 2025. Method for Measuring the Registration Efficiency of the 478 Kev Line in a gamma-ray Spectrometer. Patent for invention RU, 285742. (Accessed 13 November 2025).

Kobayashi, T., Kanda, K., 1983. Microanalysis system of ppm order B-10 concentrations in tissue for neutron capture therapy by prompt gamma-ray spectrometry. Nucl. Instrum. Methods Phys. Res. 204, 525–531. https://doi.org/10.1016/0167-5087(83)90082-0.

Sauerwein, W., Bet, P., Wittig, A., 2025. Drugs for BNCT: BSH and BPA. In: Sauerwein, W., Wittig, A., Moss, R., Nakagawa, Y., Ono, K. (Eds.), Neutron Capture Therapy: Principles and Applications, second ed. Springer, pp. 205–251.

Sauerwein, W., Wittig, A., Moss, R., Nakagawa, Y., 2012. Neutron Capture Therapy: Principles and Applications. Springer.

SEG-1KP semiconductor gamma-ray energy spectrometers. https://all-pribors.ru/opisanie/66003-16-seg-1kp-75349. (Accessed 13 January 2026).

Sycheva, T., Berendeev, E., Verkhovod, G., Taskaev, S., 2023. A single coned poly-biz moderator designed for animal irradiation in boron neutron capture therapy. Appl. Radiat. Isot. 198, 110818. https://doi.org/10.1016/j.apradiso.2023.110818.

Taskaev, S., 2024. Accelerator-Based Neutron Source VITA. FizMatLit, Moscow, p. 248.

Uspenskii, S.A., Khaptakhanova, P.A., Zaboronok, A.A., Kurkin, T.S., Volkova, O.Yu, Mechetina, L.V., Taranin, A.V., Kanygin, V.V., Matsumura, A., Taskaev, S.Yu, 2020. Elemental boron nanoparticles: production by ultrasonication in aqueous medium and application in boron neutron capture therapy. Dokl. Chem. 491, 45–48. https://doi.org/10.1134/S0012500820030027.

Zaboronok, A., Khaptakhanova, P., Uspenskii, S., Bekarevich, R., Mechetina, L., Volkova, O., Mathis, B., Kanygin, V., Ishikawa, E., Kasatova, A., Kasatov, D., Shchudlo, I., Sycheva, T., Taskaev, S., Matsumura, A., 2022. Polymer-stabilized elemental boron nanoparticles for boron neutron capture therapy: initial irradiation experiments. Pharmaceutics 14, 761. https://doi.org/10.3390/pharmaceutics14040761.